Comparison of Finite Difference and Finite Element Methods for Modeling Chloride Diffusion in Concrete

Ramin Pahnabi
Civil and Construction Engineering
Brigham Young University
Provo, United States
rpahnabi@byu.edu

W. Spencer Guthrie
Civil and Construction Engineering
Brigham Young University
Provo, United States
guthrie@byu.edu

Kendrick M. Shepherd
Civil and Construction Engineering
Brigham Young University
Provo, United States
kendrick_shepherd@byu.edu

***Abstract*—A proper understanding of chloride ion ingress into concrete and effective mitigation of its effects are crucial for preventing corrosion and premature failure of reinforced concrete structures. Previous National Institute of Standards and Technology(NIST) software employed the finite difference method (FDM) to evaluate chloride diffusion in concrete; however, this approach is not readily extensible to modeling complex geometries including the effects of reinforcing rebar. The purpose of this study is to develop finite element method (FEM) software that can exactly reproduce the FDM results, and can be extended to handle more general and complex geometries, such as concrete containing reinforcing steel (rebar). The FEM results show good agreement with the FDM results and the FEM could be used for the more complicated problem indicating little difference between both methods.**

***Index Terms*—Chloride, Finite Deference Method (FDM), Finite Element Method (FEM), Concrete, Corrosion**

I. Introduction

Chloride-induced corrosion is the main cause of deterioration of reinforced concrete (RC) structures in chloride-laden environments [1] and consequently, much research effort has been put towards the prediction of chloride-induced corrosion damage in RC structures [2]–[7]. A considerable amount of research has been undertaken on the chloride-induced corrosion process, and different types of models, including empirical, mathematical, numerical and probabilistic ones, have been developed for service life prediction of corrosion-affected RC structures [2], [3], [8]. In the past, both empirical and numerical approaches have been used to develop corrosion rate prediction models, each with its own strengths and shortcomings. Experimental models work well within the test conditions they were created for, but they often do not apply effectively to situations beyond the experiments [9]–[11]. Therefore, numerical methods are frequently used to ensure reliable prediction in general conditions. These methods include the finite difference method (FDM) and finite element method(FEM).

National Institute of Standards and Technology(NIST) historically deployed FDM software [18] used by state departments of transportation to predict chloride diffusion in concrete bridge decks [19]. While FDM provides a straightforward and computationally efficient method for modeling diffusion, it is often limited in handling complex geometries. There are many papers about the importance the FEM in chloride diffusion [12], [14]. Furthermore, studies [13] show that the FEM can be used to predict crack initiation and propagation due to chloride-induced corrosion. These results then used to update chloride propagation and predictions to realistically represent how cracking and corrosion affect each other.

In this study, we leverage FEM's flexibility to simulate chloride diffusion and validate its performance against FDM results. While FDM is straightforward for simple domains, it struggles with the geometric complexity and boundary conditions. The variational formulation and capacity of FEM to operate unstructured meshed make it inherently more flexible. The following sections demonstrate how FEM provides alternative framework for predicting chloride penetration, ultimately supporting better durability evaluation and maintenance strategies for RC infrastructure.

Furthermore, a pathway is identified to translate the existing FDM code into the expanded FEM framework, enabling more accurate and flexible modeling of real-world structural conditions.

II. Physics Problem

a) Coupled system of equations: Chloride ingress into concrete is often modeled using the coupled system of equations,

$$\begin{aligned}\frac{\partial C_{\text{free}}}{\partial t} = \frac{\partial}{\partial x}\left(D(x)\,\frac{\partial C_{\text{free}}}{\partial x}\right) - k_{\text{react}}\,r(t)\,C_{\text{free}} \\ - k_{\text{bind}}\left(\frac{\alpha C_{\text{free}}}{1+\beta C_{\text{free}}} - C_{\text{ads}}\right) + f(t), \\ 0 < x < L,\ t > 0,\end{aligned} \tag{1}$$

$$\frac{dC_{\text{react}}}{dt} = k_{\text{react}} r\left(C_{\text{react}}\right) C_{\text{free}}, \tag{2}$$

$$\frac{dC_{\text{ads}}}{dt} = k_{\text{bind}}\left(\frac{\alpha C_{\text{free}}}{1+\beta C_{\text{free}}} - C_{\text{ads}}\right), \tag{3}$$

where $C_{\text{free}}(x,t)$ denotes the free chloride concentration in the pore solution, $D(x)$ is the spatially varying diffusion coefficient, k_{react} is the reaction rate constant, $r(t)$ is a reaction indicator function that equals one in reactive regions and zero otherwise, and $f(t)$ represents a source term. The variable C_{ads} denotes the adsorbed chloride concentration (mol/m^3). The parameters k_{bind}, α, and β control the binding kinetics and adsorption capacity, while L denotes the length of the spatial domain.

The first equation represents the diffusion–reaction model governing the free chloride concentration. By neglecting the reaction term, the model reduces to the pure diffusion case (see (1)–(2)). Equation (3) represents a Langmuir-type adsorption model, which describes the binding of chloride ions to the concrete. This model couples the diffusion of free chloride ions with an adsorption process. By accounting for this adsorption term, the bound chloride is separated from the total chloride content, and the remaining portion corresponds to the free chloride concentration.

b) Boundary Conditions: The diffusion–reaction problem is closed by prescribing boundary conditions at both ends of the spatial domain. At the top boundary ($x = 0$), the chloride concentration is typically fixed to a prescribed value, representing a constant or time–dependent exposure condition. This is enforced through a Dirichlet boundary condition,

$$U(0,t) = g, \tag{4}$$

where g denotes the imposed boundary concentration.

At the bottom boundary ($x = L$), chloride transport frequently is controlled through a specified outward flux, which is modeled using a Neumann boundary condition,

$$\left.\frac{\partial U}{\partial x}\right|_{x=L} = -\,h, \tag{5}$$

where h represents the prescribed flux at the boundary which is typically 0. Together, these boundary conditions reflect a system in which chloride ingress is driven by exposure at one boundary while transport across the opposite boundary is regulated by a specified flux.

III. Numerical Methods

The coupled diffusion–reaction–adsorption system is solved using a staggered (operator-splitting) time-integration scheme, in which diffusion and reaction/adsorption are solved sequentially at each time step [17]. The Forward Euler method is used for all temporal discretization while we compute the spatial discretization with FEM.

A. Finite Difference Method (FDM)

a) Spatial Discretization (Finite Difference): The spatial domain is discretized using a one-dimensional finite difference method. The interval $[0, L]$ is divided into N uniform subintervals of size $\Delta x = L/N$, resulting in nodal points $x_i = i\,\Delta x$ for $i = 0, \ldots, N$. The solution at each node is approximated by a discrete variable $d_i(t) \approx d(x_i, t)$.

Spatial derivatives in the diffusion term are approximated using second-order central differences.

Boundary conditions are incorporated directly into the discrete system. At the top boundary, the prescribed concentration is enforced by fixing the nodal value, while at the bottom boundary, the specified flux condition is imposed through a finite difference approximation of the spatial gradient.

b) Time Discretization: Forward Euler (Explicit) Method: In the Forward Euler method, for the interior nodes we have, for $1 \le i \le N-1$,

$$d_i^{n+1} = d_i^n + \Delta t\Big[f_i - \frac{D_i(d_i^n - d_{i-1}^n) - D_{i+1}(d_{i+1}^n - d_i^n)}{\Delta x^2} - k_{\text{react}}\, r_i\, d_i^n\Big], \tag{6}$$

With boundary conditions applied explicitly: At the top surface of the concrete slab, the chloride concentration is assumed to be maintained at a fixed value, representing continuous exposure to a chloride-rich environment (considered as Dirichlet BCs). This condition enforces a constant chloride level at the exposed surface throughout the simulation. At the bottom of the slab, chloride transport is governed by a prescribed flux condition (Neumann BCs) or a constant chloride level (Dirichlet BCs). This represents controlled exchange across the lower boundary, such as limited chloride penetration into an underlying layer. By specifying the rate at which chloride enters or leaves the slab at this boundary, the model captures the physical constraint on chloride movement at the base of the domain.

Thus the explicit update at node N is:

$$d_N^{n+1} = d_N^n + \Delta t\Big[f(x_N) + \frac{2h}{\Delta x} + \frac{2D_N}{\Delta x^2}\big(d_{N-1}^n - d_N^n\big) - k_{\text{react}}\, r_N\, d_N^n\Big], \tag{7}$$

c) CFL Condition for Explicit Scheme: To be sure that the explicit method (Forward-Euler) is reliable and the results are stable, following limitation is considered:

$$\text{CFL} = \frac{\max(D)\,\Delta t}{\Delta x^2} \le 0.5 \quad \text{for stability.} \tag{8}$$

B. Finite Element Method (FEM)

a) Spatial Discretization: The one-dimensional diffusion–reaction problem is solved numerically using the finite element method (FEM) with linear basis function. The formulation follows the standard Galerkin approach described by [15]. FEM is particularly well suited for transport problems in heterogeneous materials such as concrete, as it naturally accommodates spatially varying material properties and allows for local mesh refinement [15].

In abstract form, the weak problem can be written as: find $u \in S$ such that

$$a(u,w) = \ell(w) \qquad \forall w \in V, \tag{9}$$

$$a(u,w) = \int_\Omega D\, u_{,x}\; w_{,x}\; dx, \tag{10}$$

$$\ell(w) = \int_\Omega f\, w\, dx, \tag{11}$$

where S and V denote appropriate trial and test spaces, $a(\cdot,\cdot)$ is the bilinear form associated with diffusion and reaction processes, and $\ell(\cdot)$ represents the contribution of source terms and boundary fluxes [15].

The solution field is approximated within a finite-dimensional subspace spanned by shape functions defined over a partition of the spatial domain. This leads to a discrete representation of the form:

$$u_h(x) = \sum_{i=1}^{N} d_i\, N_i(x), \tag{12}$$

where $N_i(x)$ are the finite element shape functions and d_i are the unknown nodal values(coefficients). Substituting this approximation into the weak form and choosing the test functions from the same space yields a system of algebraic equations of the form.

The Standard form is:

$$\mathbf{K}\mathbf{d} = \mathbf{F}, \tag{13}$$

where $\mathbf{K}$ is the global stiffness matrix arising from diffusion and reaction terms, $\mathbf{d}$ is the vector of nodal unknowns representing the chloride concentration ($\mathbf{C_{free}}$), and $\mathbf{F}$ contains the contributions from source terms and boundary fluxes. This system is then solved to obtain the spatial distribution of chloride concentration.

b) Time Discretization: For time-dependent problems, the semi-discrete finite element formulation leads to a system of ordinary differential equations of the form

$$\mathbf{M}\,\dot{\mathbf{d}}(t) + \mathbf{K}\,\mathbf{d}(t) + \mathbf{R}\mathbf{M}\,\mathbf{d}(t) = \mathbf{F}(t), \tag{14}$$

where $\mathbf{M}$ is the mass matrix, $\mathbf{K}$ is the diffusion stiffness matrix, $\mathbf{R}$ is the reaction matrix, $\mathbf{d}(t)$ is the vector of time-dependent nodal unknowns, and $\mathbf{F}(t)$ is the load vector.

To account for limited binding capacity, the reaction term is controlled by a binary flag $r \in \{0, 1\}$. The flag is defined as

$$r = \begin{cases} 1, & C_{free} > C_{react}, \\ 0, & C_{free} \le C_{react}, \end{cases}$$

where C_{free} and C_{react} denote the free and reacted (bound) chloride concentrations, respectively. When the reacted chloride level reaches or exceeds the free chloride, further reaction is deactivated.

The semi-discrete system becomes

$$\mathbf{M}\dot{\mathbf{d}}(t) + \mathbf{K}\mathbf{d}(t) + r\,\mathbf{M}\mathbf{d}(t) = \mathbf{F}(t). \tag{15}$$

Forward Euler Scheme: Using a Forward Euler discretization in time, the time derivative in (14) is approximated as

$$\dot{\mathbf{d}}(t^n) \approx \frac{\mathbf{d}^{n+1} - \mathbf{d}^n}{\Delta t},$$

where Δt denotes the time-step size and the superscript n indicates the discrete time level.

Substituting this approximation into (14) and solving for $\mathbf{d}^{n+1}$ yields the explicit update formula

$$\mathbf{d}^{n+1} = \mathbf{d}^n + \Delta t\, \mathbf{M}^{-1}\big(\mathbf{F}^n - \mathbf{K}\,\mathbf{d}^n - \mathbf{r}\mathbf{M}\,\mathbf{d}^n\big), \tag{16}$$

which advances the solution from time level t^n to t^{n+1}.

Equation (16) is conditionally stable and requires the time step Δt to satisfy a problem-dependent stability constraint (8).

C. Nitsche Method for Weak Imposition of Dirichlet Boundary Conditions

To weakly impose essential boundary conditions within the finite element framework, Nitsche's method is employed [16]. This approach allows Dirichlet boundary conditions to be enforced variationally, while maintaining consistency and stability of the numerical scheme. In contrast, finite difference methods (FDM) apply boundary conditions directly at grid points, making their implementation simple, especially for structured domains.

In Nitsche's method [16], the standard weak formulation is augmented by additional boundary terms that weakly enforce the Dirichlet condition. These terms ensure consistency with the strong form, restore symmetry of the bilinear form, and add a stabilization contribution controlled by a penalty parameter.

The resulting bilinear form is

$$\begin{aligned} a_{\text{Nitsche}}(u, w) = a(u, w) &- \int_{\Gamma_D} D\, u_{,x}\; w\, ds \\ &- \int_{\Gamma_D} D\, w_{,x}\; u\, ds + \int_{\Gamma_D} \frac{\gamma D}{h_e}\, u\, w\, ds, \end{aligned} \tag{17}$$

where u is the trial function, w is the test function, h_e is a characteristic boundary element length, and $\gamma > 0$ is a penalty parameter. A value of $\gamma = 100$ was used, which yielded results in agreement with the NIST software.

The associated linear functional is given by

$$\ell_{\text{Nitsche}}(w) = \ell(w) + \int_{\Gamma_D} D\, w_{,x}\; g\, ds + \int_{\Gamma_D} \frac{\gamma D}{h_e}\, g\, w\, ds, \tag{18}$$

where f is the body force and g denotes the prescribed Dirichlet boundary value.

a) Element-Level Contributions: For elements adjacent to Γ_D, the Nitsche boundary terms add the following contributions to the stiffness matrix:

$$K_{ab}^{(e)} \mathrel{+}= \int_{\Omega_e} D \left(-N_a' N_b - N_b' N_a + \frac{\gamma}{h_e} N_a N_b \right) dx, \tag{19}$$

and to the load vector:

$$F_a^{(e)} \mathrel{+}= \int_{\Omega_e} \left(-D\, N_a'\, g + \frac{\gamma D}{h_e}\, N_a\, g \right) dx, \tag{20}$$

IV. Validation and Comparison

Here we present a comparison between the finite difference method (FDM), the standard finite element method (FEM) without Nitsche's method and without mass lumping, and

a modified FEM incorporating Nitsche's method and mass lumping.

Without the use of the Nitsche method and mass lumping, the finite element results were found to be in close agreement with those obtained using the finite difference method (FDM). In the Nitsche formulation, Dirichlet boundary conditions are imposed weakly through the introduction of a penalty term parameterized by γ, rather than being enforced strongly.

When the Nitsche method is combined with mass lumping, the resulting finite element solution reproduces the FDM results exactly. This agreement provides confidence that the proposed numerical techniques do not alter the underlying physics of the problem and remain consistent with the physics-based simulation benchmarks defined by the National Institute of Standards and Technology (NIST) software.

In FEM(-ML +N), ML refers to mass lumping and N refers to Nitsche's method. A plus sign (+) indicates that the corresponding technique is used, while a minus sign (-) indicates that it is not. Using this notation, the FEM variants are as follows:

- FEM(-ML -N): without mass lumping and without Nitsche's method
- FEM(-ML +N): without mass lumping but with Nitsche's method
- FEM(+ML -N): with mass lumping but without Nitsche's method
- FEM(+ML +N): with mass lumping and with Nitsche's method

Fig. 1 shows the results on a coarse mesh, while Fig. 2 presents the corresponding comparison for a fine mesh.

The next set of figures illustrates the differences between the FEM solutions and the reference FDM solution.

Fig. 3 compares the FDM solution with all of the four FEM formulations. The Fig. 3 plot corresponds to the coarse mesh, while Fig. 4 the second corresponds to the fine mesh.

As observed in the previous figures, the discrepancy between the FDM solution and the FEM formulation using

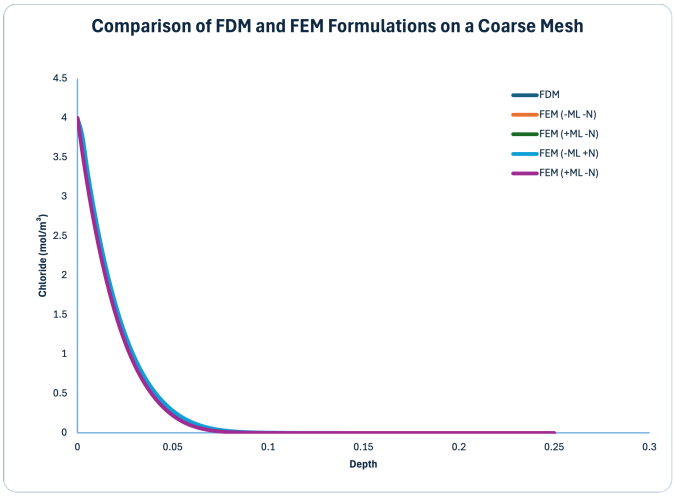

Fig. 1. Comparing FDM with FEM with Nitsche and ML with coarse mesh.

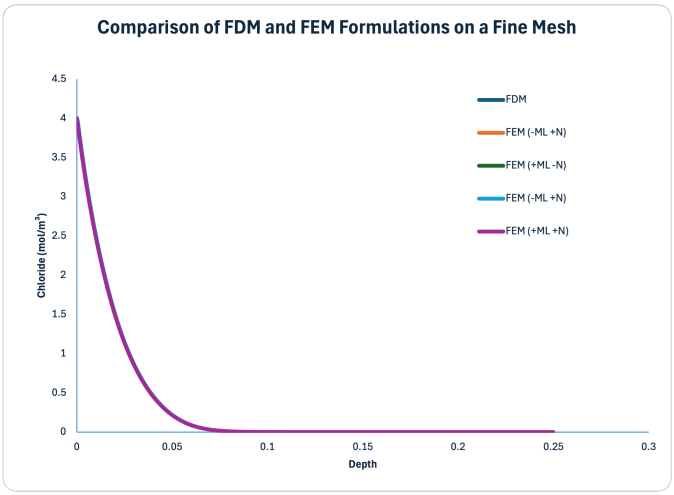

Fig. 2. Comparing FDM with FEM with Nitsche and ML with fine mesh.

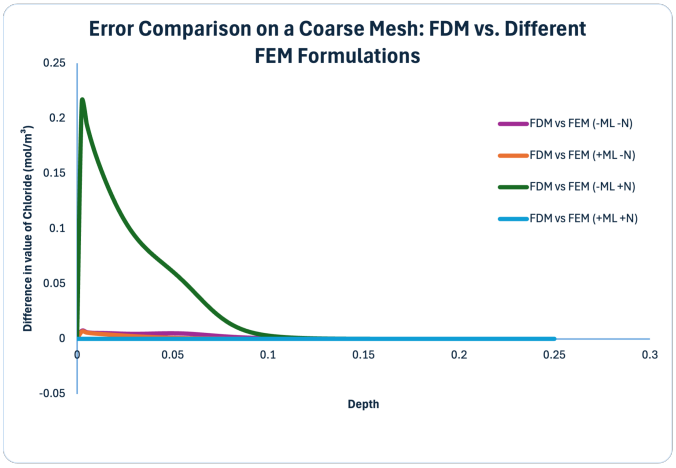

Fig. 3. Error comparison between FDM and FEM formulations on the coarse mesh.

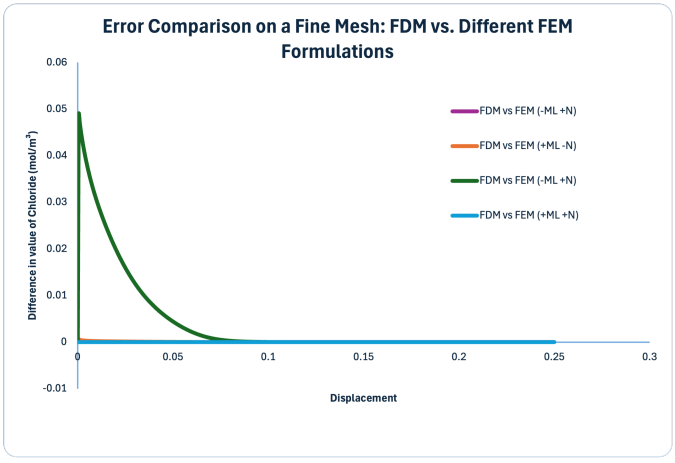

Fig. 4. Error comparison between FDM and FEM formulations on the fine mesh.

Nitsche's method without mass lumping is significantly larger

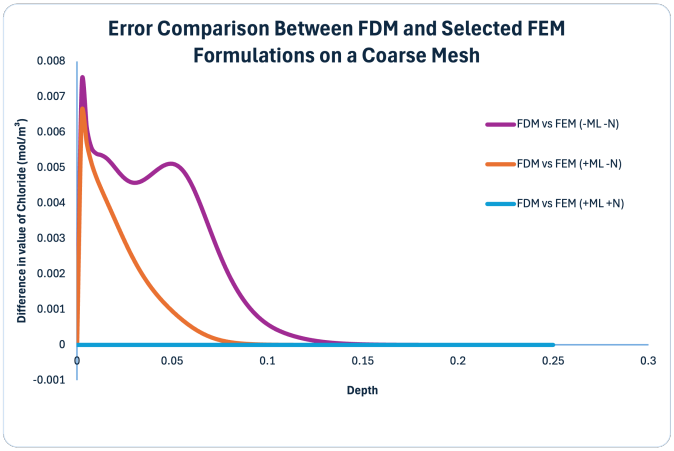

Fig. 5. Error comparison between FDM and selected FEM formulations on the coarse mesh.

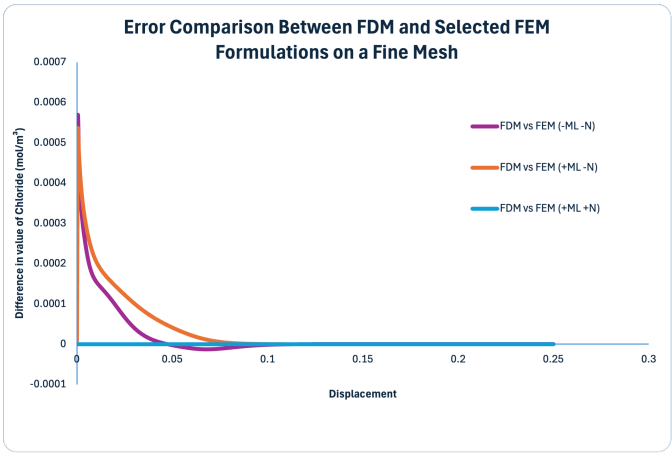

Fig. 6. Error comparison between FDM and selected FEM formulations on the fine mesh.

than the others. To improve clarity and enable a more meaningful comparison among the remaining methods, this formulation is omitted in the following plots.

Accordingly, Fig. 5 presents the comparison between the FDM solution and the three FEM formulations, excluding FEM(-ML +N). Fig. 5 corresponds to the coarse mesh, while Fig. 6 shows the results for the fine mesh.

Accordingly, we compare the coarse mesh (100 spatial layers, 500 time steps) and the fine mesh (500 spatial layers, 100 000 time steps) to assess the influence of mesh resolution on the solution. We consider the FDM solution and four FEM formulations: (i) FEM(-ML -N), (ii) FEM(+ML -N), (iii) FEM(-ML +N), and (iv) FEM(+ML +N).

Table I reports the maximum and mean absolute differences between the fine-mesh solution and the coarse-mesh solution (interpolated onto the fine grid). All methods exhibit convergence with mesh refinement. For FDM and the standard FEM formulations (with or without mass lumping), the discrepancies are of order 10^{-2} in the maximum norm and about 5×10^{-3} on average, indicating that the coarse mesh already

TABLE I
CONVERGENCE BETWEEN COARSE AND FINE MESHES: MAXIMUM AND MEAN ABSOLUTE DIFFERENCE OF THE SOLUTION .

Method	Max. abs. diff.	Mean abs. diff.
FDM	0.0389	0.00412
FEM(-ML -N)	0.0445	0.00569
FEM(+ML -N)	0.0440	0.00475
FEM(-ML +N)	0.201	0.0281
FEM(+ML +N)	0.0389	0.00412

TABLE II
MODEL PARAMETERS USED IN THE CHLORIDE INGRESS SIMULATIONS

Symbol	Description
$t_{\max}$	Maximum number of days of exposure: 1800 days
d	Thickness of the specimen: 0.25 m
WC	Water–cement ratio: 0.5
hy	Degree of hydration: 0.75
VF	Volume fraction of aggregate: 70%
AC	Air content (volume fraction): 2.0%
D_i	Time-dependent diffusivity: 6e-12
θ_i	Exterior temperature at month i of exposure: Table III.
t_{cur}	Time before exposure begins (s): 28 days
$\kappa_{\text{rel}}^{\text{surf}}$	Relative diffusivity for surface layer: 1
d_{surf}	Thickness of the surface layer: 5.0 mm
E	Activation energy for chloride diffusion: 40 kJ/mole
R	Universal gas constant: 0.008314 kJ/(mol K)
α	Binding isotherm parameter: 1.67
β	Binding isotherm parameter: 4.08
k_{bind}	Binding rate constant: 1e-07
$C3A$	C3A volume fraction (typically 5–10%)
$C4AF$	C4AF volume fraction (typically 5–13%)
$C3A_{\text{react}}$	Formation of Friedel's salt from C3A (= 7.419)
$C4AF_{\text{react}}$	Formation of Friedel's salt from C4AF (= 4.119)
k_{react}	Chloride–aluminate reaction rate: 1e-08

provides a reasonably accurate approximation.

A larger difference is observed for the FEM formulation using Nitsche's method without mass lumping (maximum difference ≈ 0.20, mean ≈ 0.028). This indicates a stronger sensitivity of this formulation to mesh resolution. When mass lumping is combined with Nitsche's method, however, the differences reduce to the same level as the other methods. Overall, these results confirm the convergence of all approaches while highlighting the improved stability and mesh robustness obtained by combining Nitsche's method with mass lumping.

The same domain and parameters are considered for FDM and FEM. Some of them are listed in Table II.

V. DISCUSSION

A. Advantages of FEM over FDM

The finite element method (FEM) offers several advantages over the finite difference method (FDM), particularly for engineering applications including complex geometries and boundary conditions. Unlike standard FDM, which is typically restricted to structured grids and regular domains, FEM can naturally accommodate irregular geometries and spatially varying material properties. In addition, FEM provides greater flexibility in the treatment of complex boundary conditions and is generally more suitable for solving problems involving

TABLE III
MONTHLY CHLORIDE CONCENTRATION AND TEMPERATURE VALUES USED IN THE SIMULATION.

Month	Cl^-	Temperature (K)
0	4.0000	278.15
1	4.0000	278.15
2	4.0000	288.15
3	4.0000	288.15
4	4.0000	293.15
5	4.0000	298.15
6	4.0000	303.15
7	4.0000	303.15
8	4.0000	298.15
9	4.0000	293.15
10	4.0000	288.15
11	4.0000	283.15

complicated physical processes. As a result, complex problems can often be modeled more effectively using FEM than FDM.

B. Limitations

Despite their effectiveness, both FEM and FDM require careful treatment of boundary conditions and discretization parameters to ensure numerical accuracy and stability. The FDM is computationally efficient and simple to implement, but its applicability is limited for irregular domains and complex geometries. On the other hand, while FEM provides greater flexibility and modeling capability, it typically involves higher computational cost and increased implementation complexity compared to FDM.

VI. CONCLUSIONS

In this study, the finite element method (FEM) was applied to simulate one-dimensional chloride diffusion and its performance was compared with the finite difference method (FDM). The results show that, with appropriate boundary treatment, such as the use of Nitsche's method and mass lumping, the FEM solutions closely reproduce the reference FDM results. The results of the FEM(+ML +N) are still comparable for the considered diffusion problem.

In addition to its accuracy, FEM offers greater flexibility for modeling complex engineering problems in reinforced concrete. In particular, it allows the treatment of irregular geometries, spatially varying material properties, and more sophisticated boundary conditions, which are difficult to handle using standard FDM approaches.

Potential extensions: The present study motivates the extension of the FEM analysis for chloride diffusion in many directions, including 2D and 3D analysis, alternative temporal discretization extension to cracking to advective flow.

REFERENCES

[1] M. Otieno, H. Beushausen, and M. Alexander, "Chloride-induced corrosion of steel in cracked concrete—Part II: Corrosion rate prediction models," Cement and Concrete Research, Vol. 41, No. 4, pp. 443–452, 2011.

[2] U. M. Angst, E. Rossi, C. Boschmann Käthler, D. Mannes, P. Trtik, B. Elsener, Z. Zhou, and M. Strobl, "Chloride-induced corrosion of steel in concrete—insights from bimodal neutron and X-ray microtomography combined with ex-situ microscopy," Materials and Structures, 2024.

[3] M. Otieno, H. Beushausen, and M. Alexander, "Chloride-induced corrosion of steel in cracked concrete—Part I: Experimental studies under accelerated and natural marine environments," Cement and Concrete Research, 2015.

[4] C. S. Das, H. Zheng, and J.-G. Dai, "A review of chloride-induced steel corrosion in coastal reinforced concrete structures: Influence of microclimate," Construction and Building Materials, 2024.

[5] C. Liang, Z. Cai, H. Wu, J. Xiao, Y. Zhang, and Z. Ma, "Chloride transport and induced steel corrosion in recycled aggregate concrete: A review," Construction and Building Materials, 2021.

[6] J. Němeček, P. Trávníček, J. Němečková, and J. Kruis, "Mitigation of chloride induced corrosion in reinforced concrete structures and its modeling," Computers and Concrete, 2021.

[7] S. C. Paul and G. P. A. Greeff van Zijl, "Corrosion deterioration of steel in cracked SHCC," International Journal of Concrete Structures and Materials, 2017.

[8] J. Zhang and M. M. S. Cheung, "Modeling of chloride-induced corrosion in reinforced concrete structures," Materials and Structures, Vol. 45, No. 10, pp. 1555–1566, 2012.

[9] P. Li, C. Li, C. Jia, and D. Li, "A comparative study on chloride diffusion in concrete exposed to different marine environment conditions," Cement and Concrete Composites, 2024.

[10] P. Su, Q. Dai, and E. S. Kane, "Predicting chloride ingression in concrete containing different SCMs based on chloride binding and electrical resistivity," Construction and Building Materials, 2024.

[11] T. Ferenc, E. Wojtczak, B. Meronk, J. Ryl, K. Wilde, and M. Rucka, "Characterization of corrosion-induced fracture in reinforced concrete beams using electrical potential, ultrasound and low-frequency vibration," Construction and Building Materials, 2023.

[12] J. Xiao, J. Ying, and L. Shen, "FEM simulation of chloride diffusion in modeled recycled aggregate concrete," Construction and Building Materials, Vol. 29, pp. 12–23, 2012.

[13] E. Redaelli, L. Bertolini, W. Peelen, and R. Polder, "FEM-models for the propagation period of chloride induced reinforcement corrosion," Materials and Corrosion, Vol. 57, No. 8, pp. 628–635, 2006.

[14] E. Korec, M. Jirásek, H. S. Wong, and E. Martínez-Pañeda, "A phase-field chemo-mechanical model for corrosion-induced cracking in reinforced concrete," Mechanics of Materials, 2023.

[15] T. J. R. Hughes, The Finite Element Method: Linear Static and Dynamic Finite Element Analysis. Upper Saddle River, NJ: Prentice Hall, 2000.

[16] E. Burman, "A consistent Nitsche formulation for the weak imposition of boundary conditions in convection–diffusion problems," Computer Methods in Applied Mechanics and Engineering, vol. 199, no. 47–48, pp. 2845–2855, 2010.

[17] D. Lanser and J. G. Verwer, "Analysis of operator splitting for advection–diffusion–reaction problems from air pollution modelling," Journal of Computational and Applied Mathematics, vol. 111, no. 1–2, pp. 201–216, 1999.

[18] A. W. Birdsall, W. S. Guthrie, and D. P. Bentz, "Effects of initial surface treatment timing on chloride concentrations in concrete bridge decks," Transp. Res. Rec., vol. 2028, no. 1, pp. 103–110, 2007.

[19] W. S. Guthrie and A. W. Birdsall, *Effect of initial surface treatment timing on chloride concentrations in concrete bridge decks*, Tech. Rep., 2008.